

Published in final edited form as:

*J Mol Cell Cardiol.* 2010 April ; 48(4): 600–608. doi:10.1016/j.yjmcc.2009.11.006.

## Nesprin-1 mutations in human and murine cardiomyopathy

Megan J. Puckelwartz<sup>1,\*</sup>, Eric J. Kessler<sup>2,\*</sup>, Gene Kim<sup>2</sup>, Megan M. DeWitt<sup>2</sup>, Yuan Zhang<sup>2</sup>, Judy U. Earley<sup>2</sup>, Frederic F.S. Depreux<sup>2</sup>, James Holaska<sup>2</sup>, Stephanie K. Mewborn<sup>2</sup>, Peter Pytel<sup>3</sup>, and Elizabeth M. McNally<sup>1,2</sup>

<sup>1</sup>Department of Human Genetics, The University of Chicago, Chicago, IL

<sup>2</sup>Department of Medicine, Section of Cardiology, The University of Chicago, Chicago, IL

<sup>3</sup>Department of Pathology, The University of Chicago, Chicago, IL

### Abstract

Mutations in *LMNA*, the gene encoding the nuclear membrane proteins, lamins A and C, produce cardiac and muscle disease. In the heart, these autosomal dominant *LMNA* mutations lead to cardiomyopathy frequently associated with cardiac conduction system disease. Herein, we describe a patient with the R374H missense variant in nesprin-1 $\alpha$ , a protein that binds lamin A/C. This individual developed dilated cardiomyopathy requiring cardiac transplantation. Fibroblasts from this individual had increased expression of nesprin-1 $\alpha$  and lamins A and C, indicating changes in the nuclear membrane complex. We characterized mice lacking the carboxy-terminus of nesprin-1 since this model expresses nesprin-1 without its carboxy-terminal KASH domain. These  $\Delta/\Delta$  KASH mice have a normally assembled but dysfunctional nuclear membrane complex and provide a model for nesprin-1 mutations. We found that  $\Delta/\Delta$  KASH mice develop cardiomyopathy with associated cardiac conduction system disease. Older mutant animals were found to have elongated P wave duration, elevated atrial and ventricular effective refractory periods indicating conduction defects in the myocardium, and reduced fractional shortening. Cardiomyocyte nuclei were found to be elongated with reduced heterochromatin in the  $\Delta/\Delta$  KASH hearts. These findings mirror what has been described from lamin A/C gene mutations and reinforce the importance of an intact nuclear membrane complex for a normally functioning heart.

### Keywords

cardiomyopathy; nuclear membrane; lamin A/C; nesprin

### INTRODUCTION

The LINC complex links the nucleus to the cytoplasm by bridging the network of intermediate filaments inside the nucleus through the double membranes of the nuclear membrane and to the cytoplasm [1]. The nuclear lamins line the inner face of the nuclear membrane forming a

© 2009 Elsevier Ltd. All rights reserved

To whom correspondence should be addressed: E. M. McNally The University of Chicago 5841 S. Maryland, MC6088 Chicago, IL 60637 T: 773 702 2672 F: 773 702 2681 emcnally@uchicago.edu.

\* Authors contributed equally to this work.

**Publisher's Disclaimer:** This is a PDF file of an unedited manuscript that has been accepted for publication. As a service to our customers we are providing this early version of the manuscript. The manuscript will undergo copyediting, typesetting, and review of the resulting proof before it is published in its final citable form. Please note that during the production process errors may be discovered which could affect the content, and all legal disclaimers that apply to the journal pertain.

**DISCLOSURES** The authors have no conflicts of interest relevant to the conduct and presentation of this research.

structural attachment to the LINC complex. The LINC complex contains the nesprins situated on both the inner and outer nuclear membrane. The largest nesprin isoforms localize to the outer nuclear membrane where they bind actin at their amino-terminus in the cytoplasm. The short forms of nesprin localize to the outer and inner nuclear membrane. At the inner nuclear membrane they directly interact with the intermediate filaments lamins A and C. The SUN proteins span the lumen between the inner and outer nuclear membrane and link the nesprins through the carboxy-terminal domain of nesprin [1–3]. The SUN proteins also bind directly to lamin A/C [4]. Lamins A and C are both produced from the *LMNA* gene. Lamins A and C are widely expressed type V intermediate filaments that, together with other lamin-associated proteins at the inner nuclear membrane, provide structure to the nucleus and play a role in chromatin organization and gene regulation [5–7].

Over 300 different mutations have been described in *LMNA*, and cardiac disease is a prominent component. Cardiomyopathy from *LMNA* mutations can occur in isolation or may be associated with progressive muscle weakness in the form of Emery-Dreifuss muscular dystrophy (EDMD). Whether associated with muscle disease or not, cardiomyopathy with *LMNA* gene mutations is frequently associated with cardiac conduction system disease that includes sinus node disease, atrial fibrillation, atrioventricular heart block and both tachyarrhythmias and bradyarrhythmias [8–11]. Structural heart disease may be associated with *LMNA* gene mutations and typically includes dilatation of the left ventricle and compromised systolic function and heart failure. With *LMNA* conduction system disease, generally, the atrioventricular node is most affected preventing conduction from the atria to the ventricles. However, the disease is not limited to the atrioventricular node or ventricle as some patients develop sinus bradycardia or atrial fibrillation. Morbidity and mortality from *LMNA* gene mutations is often attributed to conduction system disease. It is estimated that greater than 40% of patients may die suddenly as a result of ventricular arrhythmias; therefore, implantation of a cardioverter-defibrillator has been recommended to prevent sudden cardiac death [8,10,12,13].

While mutations in *LMNA* are generally autosomal dominant, mutations in another LINC complex protein, emerin, cause an X-linked form of EDMD. The cardiac defects seen in X-linked EDMD are very similar to those seen in *LMNA* patients. Emerin is a 34kDa protein anchored to the inner nuclear membrane through a carboxy-terminal transmembrane domain. Emerin contains a LEM domain, so named for its presence in three inner nuclear membrane proteins, lamin-associated protein, emerin and MAN-1. The LEM domain binds directly to BAF, a small protein that binds directly to chromatin [14,15]. Through this interaction, emerin participates in the LINC complex, linking the cytoplasm to the nucleus [16].

Recently, DNA variants in genes encoding the LINC complex proteins, nesprin-1 and -2, were found associated with an EDMD-like phenotype including cardiomyopathy [17]. The phenotype seen in four unrelated, small kindreds was highly variable and ranged from increased creatine kinase levels to severe dilated cardiomyopathy requiring a heart transplant in the third decade of life [17]. Two missense variants were described for nesprin-1, and these amino acid substitutions map to the more carboxy terminal regions of nesprin-1. Another missense variant was identified in the nuclear membrane isoform of nesprin-2, nesprin-2 $\beta$ . Nesprin-1 and -2 are spectrin-repeat containing proteins that through alternate initiation and splicing exist as multiple isoforms [18–21]. The largest isoforms of nesprin are approximately 1 megaDalton in size and bind actin at their amino-terminus. The carboxy-terminus of nesprin contains a KASH domain, so named for its Klarsicht, ANC-1 and Syne homology, that is approximately 60 amino acids in length including the transmembrane domain followed by a luminal domain residing in the space between the inner and outer nuclear membrane. The largest isoforms of nesprin are located at the outer nuclear membrane. The smaller isoforms contain spectrin-repeats and the KASH domain and are found within the nucleus. Nesprin-1 $\alpha$  is a short isoform

located at the inner nuclear membrane and is highly expressed in skeletal and cardiac muscle [18,21].

We recently described a mouse model of EDMD lacking the KASH domain of nesprin-1 [22]. This  $\Delta/\Delta$ KASH mouse is deleted for the carboxy-terminal KASH domain [22]. The mutation in this mouse model disrupts the LINC complex since the KASH domain is no longer available to bind SUN proteins. The phenotype of the  $\Delta/\Delta$ KASH mouse includes progressive muscle weakness, kyphoscoliosis and altered gait, all characteristics of EDMD. Here we describe a human patient with a nesprin-1 variant, located in the 1 $\alpha$  isoform that is highly expressed in heart and skeletal muscle. This individual developed severe dilated cardiomyopathy and required transplant in the third decade of life. Patient-derived fibroblasts displayed increased nesprin-1 $\alpha$  and lamins A and C protein, indicating a perturbation of the LINC complex. Due to the limited nature of patient tissue, we characterized the cardiac phenotype of the  $\Delta/\Delta$ KASH mouse model to determine whether nesprin-1 was important for cardiac function. We found that the  $\Delta/\Delta$ KASH mice develop a progressive cardiomyopathy associated with reduced fractional shortening. Moreover, electrophysiologic studies revealed that the  $\Delta/\Delta$ KASH mice have conduction defects affecting the atria and ventricular tissue. We conclude that the  $\Delta/\Delta$ KASH mouse provides a useful model for studying the cardiac dysfunction associated with mutations in the LINC complex.

## MATERIALS AND METHODS

### Patient Recruitment

Informed consent was obtained according to the guidelines of the University of Chicago's Institutional Review Board. A panel, biased toward familial inheritance of disease, of 46 unrelated patients with nonischemic cardiomyopathy and 17 with muscle disease were screened for nesprin-1 $\alpha$  mutations. The panel was composed of Caucasian subjects. The control panel was purchased from Coriell and consisted of Caucasian samples. PolyPhen analysis was performed through the portal <http://genetics.bwh.harvard.edu/pph/> using full length nesprin-1 $\alpha$ .

### Cell Lines

A fibroblast cell line was derived from skin of the patient. A normal control fibroblast cell line was obtained from American Type Culture Collection (ATCC), cell line CRL-2565. Both the patient and the control cell line were used between passage 2–7. Written, informed consent from all human subjects was obtained in accordance with the University of Chicago's Institutional Review Board.

### Tissue Culture

Dermal fibroblast cells from the patient and a normal control (ATCC line CRL-2565) were grown in MEM (supplemented with 20% fetal bovine serum).

### Genetic Analysis

DNA was extracted from blood using the PureGene kit according to the manufacturer's instructions (Qiagen). DHPLC analysis was performed on a WAVE (Transgenomic); exon 8 was analyzed at 57.5° C. SSCP was carried out using MDE (FMC) as described [23]. Direct sequencing of PCR products was conducted using cycle sequencing.

### Mice

$\Delta/\Delta$ KASH mice are homozygous for a nesprin-1 allele with an alternate carboxy-terminus. Mice were bred and genotyped as described [22].

## Immunoblotting and Immunofluorescence Microscopy

Total supernatant from 100,000 cells was analyzed for the fibroblast lines. Dermal fibroblasts from the patient and control lines (passage 2–7) were trypsinized and counted and lysed in cell lysis buffer as below. Fibroblast immunoblots were performed in triplicate. Hearts from  $\Delta/\Delta$  KASH and wildtype littermates <32 weeks old were dounce homogenized in cell lysis buffer (10mM Tris pH 7.0, 1mM EDTA pH 8.0, 150mM NaCl, 1% TritonX100) with protease inhibitors (Complete protease inhibitor mixture, Roche Molecular Biochemicals). Heart lysate protein concentration was determined using a Bio-Rad protein assay and 25  $\mu$ g of total protein was analyzed by immunoblotting. For immunoblots, the AN1 antibody [21] was used at 1:10,000. Anti-lamin A/C (Santa Cruz SC-6215) was used at 1:5000. Secondary antibody conjugated to horseradish peroxidase (Jackson Immunochemicals) was used at 1:5000. ECL-Plus (Amersham Biosciences) was used for detection and visualized on Kodak Biomax MS film.

Dermal fibroblasts from the patient and control line were grown on glass coverslips and fixed with ice-cold methanol. Hearts from 9–12 month old  $\Delta/\Delta$  KASH mice and wildtype littermates was harvested and frozen in liquid nitrogen-cooled isopentane. Frozen 7 $\mu$ m sections were fixed in ice-cold methanol for two minutes, rinsed in PBS and blocked with 5% FBS in PBS with 0.1% Triton for 1 hour at room temperature. Primary antibodies used were: AN1 1:100 and anti-Lamin A/C 1:250 (SC 20681 Santa Cruz). Sections were incubated with primary antibody in blocking buffer at 4°C overnight. Secondary antibodies conjugated to either Cy3 or Alexa 488 were incubated at room-temperature for 1 hour, sections were mounted in Vectashield with 4',6-diamidino-2-phenylindole (DAPI) (Vector Labs) and images were captured with an Axiophot microscope and iVision-Mac (BioVision Technologies) software.

## Surface electrocardiography and electrophysiology

Study animals were anesthetized with inhaled isoflurane delivered through a nosecone. ECG monitoring was maintained throughout the procedure through subcutaneous needles placed in each limb. The ECG channels were filtered between 5 and 100 Hz. In order to prevent hypothermia during prolonged procedures a warming light was used to maintain body temperature. A jugular vein cutdown was performed and after the vein was isolated a venotomy was made for direct endovascular access. A 2 french octapolar catheter was advanced down into position in the right atrium and ventricle for the electrophysiologic study. Electrograms were recorded with a BioAmp and Powerlab system with Chart5 software (ADInstruments). Bipolar pacing and extrastimuli were delivered via a Bloom stimulator. Intracardiac electrograms were filtered between 1 Hz and 500 Hz and surface ECG was filtered between 5 Hz and 100 Hz. Surface ECG intervals were recorded at the outset of each study and the QT was corrected using Bazett's. At the outset of each study the pacing output was set to twice diastolic threshold. Standard clinical electrophysiological pacing protocols were employed to determine electrophysiologic properties. Refractory periods were determined using drive trains with CL of 100 msec.

## Echocardiography

All animals were anaesthetized with isoflurane gas and the hair from the anterior chest wall was removed with a shaver and a chemical hair remover. The animals were maintained lightly anaesthetized with an isoflurane dose of 1% in room air, resulting in a heart rate of approximately 450 beats/min. Heart rate and temperature were monitored throughout the studies. Ultrasound transmission gel was applied liberally on the anterior chest wall before scanning. Studies were performed using a VisualSonics Vevo 770 High Resolution Imaging System with a 40 MHz probe. Two-dimensional images are recorded in parasternal long- and short-axis projections with guided M-mode recordings at the midventricular level in both views. Left ventricular (LV) cavity size and wall thickness are measured in at least three beats

from each projection and averaged. LV wall thickness [interventricular septum (IVS) and posterior wall (PW) thickness] and internal dimensions at diastole and systole (LVIDd and LVIDs, respectively) are measured. LV fractional shortening  $[(LVIDd - LVIDs)/LVIDd]$ , relative wall thickness  $[(IVS \text{ thickness} + PW \text{ thickness})/LVIDd]$ , and LV mass  $[1.05 (IVS \text{ thickness} + LVIDd + PW \text{ thickness})^3 - LVIDd^3]$  are calculated from the M-mode measurements.

## Histology

Mice were sacrificed and hearts were removed, immersion fixed in 10% formalin and embedded in paraffin. Coronal sections were stained with hematoxylin & eosin. Images were taken from longitudinally oriented myocardium in anatomically comparable areas. Nuclei length was measured using iVision software (BioVision Technologies).

## Electron Microscopy

Hearts from young (<32 weeks)  $\Delta/\Delta$ KASH and wildtype littermates were immersion fixed in 2.5% glutaraldehyde for at least 24 hours at 4°C. Tissues were osmicated and embedded in Epon resin and sectioned for toluidine blue stained semi-thin sections (0.5 $\mu$ m). Representative areas of longitudinally oriented cardiac muscle were selected for thin sectioning and subsequent electron microscopy (Philips CM10). Representative longitudinally oriented cardiac nuclei were photographed at either 5800 or 7900 magnification. Electron-dense heterochromatin was quantified using Image J software. Each nucleus was outlined and the mean pixel intensity was calculated. Four wildtype and five  $\Delta/\Delta$ KASH animals were scored; approximately 15 nuclei were scored for each animal.

## Statistical analyses

Significance was assessed using unpaired t-test as suggested by the distribution of data and comparisons to be made (Prism, GraphPad Software). Data are presented as mean  $\pm$  SEM.

# RESULTS

## A mutation in nesprin-1 associated with dilated cardiomyopathy

In order to determine if nesprin-1 mutations associate with dilated cardiomyopathy, we screened patients with or without muscle disease with no known mutations in lamin A/C. A panel of 46 unrelated patients with nonischemic cardiomyopathy was screened. Of these, 17 (37%) had evidence of muscle disease. We screened the 19 exons at the 3' end of nesprin-1 since these exons encode nesprin-1 $\alpha$ , the isoform highly expressed in skeletal and cardiac muscle. We identified one variant, G1316A in exon 8 of nesprin-1 $\alpha$ . This sequence variation is predicted to change the amino acid sequence from arginine to histidine at amino acid 374 (R374H). In the nesprin-1 $\alpha$  isoform, amino acid 374 is found at the end of spectrin repeat 3 and before the broken LEM-like domain [24], (Figure 1A). *In vitro* assays show that this region binds lamin A and therefore may be important in the functioning of the LINC complex [24]. Residue 374 is highly conserved across vertebrates including human, mouse, frog, and zebrafish nesprin-1 sequences (Figure 1B). PolyPhen modeling the R374H variant resulting a position specific independent counts (PSIC) score of 1.5, indicative of a possibly damaging mutation. This variant was not found in 300 ethnically-matched Caucasian control human chromosome. Sequencing revealed that the individual was heterozygous for the G1316A nucleotide change (Figure 2A). No mutations in LMNA were found in this individual. This individual underwent cardiac transplantation at 26 years of age. The proband had severe left ventricular systolic dysfunction with a reduced fractional shortening of 4.4% and left ventricular dilation as assessed by echocardiography. He had no skeletal muscle involvement. The proband's father died at 61 years of age from heart failure (Figure 2B) but his DNA sample

and DNA samples from his family members were unavailable. His father had received a pacing defibrillator, consistent with conduction system disease. The rare nature of this variant and its conservation and positioning suggest that it is causative of dilated cardiomyopathy (DCM) in the patient.

### Altered expression of LINC complex

We sought to determine the consequences of nesprin-1 $\alpha$  R374H on the structure of the LINC complex *in vivo*. Although cardiac material was not available, dermal fibroblasts were obtained from the R374H nesprin-1 $\alpha$  individual and the fibroblasts were cultured. Immunostaining with anti-nesprin-1 and anti-lamin A/C antibodies was performed alongside a control fibroblast cell line, CRL-2565, derived from an adult male and similarly studied at early passage. Both nesprin-1 and lamin A/C localized normally in the R374H patient fibroblasts, although there was some suggestion of increased expression (Figure 2). We performed immunoblotting on equal numbers of cells from the R374H and control cell lines using anti-nesprin-1 and anti-lamin A/C antibodies. Figure 2D shows that in the R374H fibroblasts, both nesprin-1 $\alpha$  and lamin A/C are found in higher levels versus the control line. Densitometry was performed to compare the levels of nesprin-1 $\alpha$  and lamins A and C in the R374H fibroblasts versus the control line. Figure 2E shows that nesprin-1 $\alpha$  is approximately four fold higher in the R374H fibroblasts versus control ( $275 \pm 84.5$  versus  $1126 \pm 216.3$ ; control and R374H respectively,  $p < 0.05$ ,  $n=3$ ). Densitometry also showed that lamins A and C are approximately two to three fold higher in the patient line (lamin A;  $1387 \pm 724$  versus  $3983 \pm 1192$ ; control and R374H, respectively,  $p < 0.05$ ,  $n=3$ ; lamin C;  $1362 \pm 628$  versus  $3516 \pm 932$ ; control and R374H, respectively,  $p < 0.05$ ,  $n=3$ ). Together these data indicate that the R374H nesprin-1 mutation perturbs the LINC complex.

### $\Delta/\Delta$ KASH mice have a disrupted LINC complex

As only a limited number of patients from small nuclear families have been identified with nesprin-1 or -2 mutations, it is difficult to assert that these variants cause DCM. We recently created a mouse model lacking the carboxy-terminus of nesprin-1 [22]. The  $\Delta/\Delta$ KASH mouse has an EDMD-like phenotype including poor muscle function and small, irregular skeletal muscle fibers. Absence of the KASH domain prevents nesprin-1 binding to SUN proteins, thereby disrupting the LINC complex [2,22]. We analyzed the localization of the LINC complex in  $\Delta/\Delta$ KASH hearts using immunostaining with anti-nesprin-1 and anti-lamin A/C antibodies, finding normal nuclear localization of the LINC components (Supplementary Figure 1A). Immunoblotting  $\Delta/\Delta$ KASH heart and littermate lysates showed equal levels of nesprin-1 and lamin A/C proteins in the  $\Delta/\Delta$ KASH and controls (Supplementary Figure 1B). Emerin, SUN1 and SUN2 were also unchanged (data not shown). These data are consistent with the findings in  $\Delta/\Delta$ KASH skeletal muscle [22] and reflect a disrupted connection between SUN2 and nesprin-1 $\alpha$ . In contrast, we expect the nesprin-1 R374H patient variant differs because it perturbs an alternative interaction within the LINC complex, rather than specifically altering the SUN2 interaction, an interaction known to rely on the KASH domain. Nonetheless, both the loss of the KASH domain and R374H variant are associated with cardiomyopathy, consistent with a role for the LINC complex in normal cardiac function. Because of the association of nesprin-1 mutations with cardiac disease, we further characterized cardiac features in  $\Delta/\Delta$  KASH mice.

### $\Delta/\Delta$ KASH mice have an elongated P duration

Surface electrocardiograms (ECG) were performed on anesthetized wildtype and  $\Delta/\Delta$ KASH mice. Two cohorts of mice were tested; one was composed of mice <32 weeks of age and the second cohort reflected older animals, >52 weeks of age. Both cohorts included males and females. Our previous studies on  $\Delta/\Delta$ KASH mice revealed that younger mice do not have

kyphoscoliosis or overt histological muscle pathology, while mice over 52 weeks have overt muscle disease. We therefore tested both groups to determine age of onset of cardiac disease. Both age cohorts exhibited a long P duration compared to littermate wildtype controls; <32 weeks: wildtype  $17.3 \pm 0.5$  n=6,  $\Delta/\Delta$ KASH  $23.8 \pm 1.4$  n=6 p=0.0009; >52 weeks: wildtype  $15.6 \pm 1.0$  n=8,  $\Delta/\Delta$ KASH  $21.4 \pm 2.1$  n=8 p=0.03 (Table 1). Neither the QRS nor the QTc were significantly different between wildtype and  $\Delta/\Delta$ KASH in either age group. However, when only older male mice were analyzed, the QRS duration was elongated in  $\Delta/\Delta$ KASH compared to wildtype (male mice, >52 weeks of age, wildtype  $13.0 \pm 0.9$  n=4,  $\Delta/\Delta$ KASH  $18.5 \pm 1.5$  n=4; p=0.02). No other sex differences were noted.

### **$\Delta/\Delta$ KASH mice have atrial myocyte conduction defects**

To study further the conduction defects of the  $\Delta/\Delta$ KASH mice, intracardiac electrophysiologic recordings were performed in both young (<32 weeks) and old (>52 weeks)  $\Delta/\Delta$ KASH mice and wildtype littermates. The atrial effective refractory period (AERP) was measured in both young (<32 weeks) and old (>52 weeks)  $\Delta/\Delta$ KASH mice and wildtype littermates. A representative surface ECG and corresponding intracardiac electrophysiologic tracing from an old (>52 weeks)  $\Delta/\Delta$ KASH mouse are shown in Figure 3A. The old (>52 weeks)  $\Delta/\Delta$ KASH mice have an AERP of  $61.2 \pm 4.8$  ms n=8 versus  $43.7 \pm 2.6$  ms n=8 in wildtype littermates (p=0.006) (Figure 3C). Young  $\Delta/\Delta$ KASH mice (<32 weeks) were also significantly different from wildtype littermates for AERP,  $45.7 \pm 2.0$  ms n=7 and  $35.0 \pm 3.4$  ms n=6, respectively (p=0.01) (Figure 3B). Ventricular effective refractory period (VERP) was also tested in both age groups. In aged (>52 weeks)  $\Delta/\Delta$ KASH mice, the VERP was  $58.7 \pm 4.8$  ms n=8 compared to  $43.75 \pm 5.6$  ms n=8 in wildtype littermates (p=0.06) (Figure 3C). Young  $\Delta/\Delta$ KASH mice (<32 weeks) were not significantly different from wildtype littermates for VERP,  $52.0 \pm 4.9$  ms n=5 and  $48.3 \pm 3.1$  ms n=6 for  $\Delta/\Delta$ KASH mice and wildtype littermate controls, respectively. While the VERP is not significant for mice >52 weeks, there is a trend for a worsening ventricular response as the  $\Delta/\Delta$ KASH mice age. No atrial fibrillation was noted during this study. Together, the elongation of both the AERP and VERP indicate that the  $\Delta/\Delta$ KASH mice have conduction defects in the myocardium of both the atria and the ventricle. The atrial defects appear earlier than the ventricular defects mimicking the conduction defects often described in patients with DCM with conduction system disease [10].

### **$\Delta/\Delta$ KASH mice have reduced fractional shortening**

To determine if the  $\Delta/\Delta$ KASH mice have reduced systolic function, M-mode transthoracic echocardiography was performed on both young (<32 weeks) and old (>52 weeks)  $\Delta/\Delta$ KASH and wildtype littermates. A representative echocardiogram is shown for an old (>52 weeks)  $\Delta/\Delta$ KASH mouse and wildtype littermate (Figure 4A). The  $\Delta/\Delta$ KASH mouse has reduced systolic function as evidenced by a reduction in fractional shortening. Young (<32 weeks)  $\Delta/\Delta$ KASH mice do not have reduced fractional shortening compared to wildtype littermates,  $52.5 \pm 2.9$ , n=5, and  $52.7 \pm 3.2$ , n=5,  $\Delta/\Delta$ KASH and wildtype, respectively (Figure 4B, top). However, as the  $\Delta/\Delta$ KASH mice age, their fractional shortening becomes significantly reduced compared to wildtype littermates,  $33.3 \pm 3.4$  n=6 and  $47.8 \pm 2.2$  n=6,  $\Delta/\Delta$ KASH and wildtype, respectively, p=0.005 (Figure 4B, bottom). Our studies did not reveal any sex differences in either the old or young cohorts. We also did not find significant differences in left ventricular end diastolic or systolic diameter in either young or old mice when adjusted for body weight (Supplementary Table 1). The severely reduced fractional shortening mimics the reduced systolic function seen in patients with DCM with conduction system defects.

### **$\Delta/\Delta$ KASH mice have abnormal elongation of cardiomyocyte nuclei**

Mutations in lamin A/C have been associated with aberrantly shaped cardiomyocyte nuclei [25,26]. We examined nuclei in the  $\Delta/\Delta$ KASH mice and found that they also have an abnormal,

elongated shape when compared to wildtype littermates (Figure 5). We measured nuclear length in cardiomyocytes from 3 animals of each genotype and age group; approximately 100 nuclei per animal were measured. In old (>52 weeks) animals,  $\Delta/\Delta$ KASH mice have significantly longer nuclei than their wildtype littermates,  $18.1 \pm 0.38 \mu\text{m}$  and  $13.5 \pm 0.21 \mu\text{m}$ , respectively,  $p=0.0001$  (Figure 5B, bottom). In young (<32 weeks) animals we also found a significant difference in nuclei length,  $16.6 \pm 0.34 \mu\text{m}$  and  $13.6 \pm 0.20 \mu\text{m}$ ,  $\Delta/\Delta$ KASH and wildtype, respectively,  $p=0.0001$ . The increased cardiomyocyte nuclei length in young animals without overt cardiac defects indicates that the malformation of the nucleus precedes the clinical disease and is the result of very early disease processes.

### **The $\Delta/\Delta$ KASH cardiomyocyte nucleus is abnormally shaped and has reduced heterochromatin**

In order to further investigate the shape of the  $\Delta/\Delta$ KASH nuclei, we performed electron microscopy on heart sections from young (<32 weeks)  $\Delta/\Delta$ KASH mice and wildtype littermates. Gross analysis of the sections reveals that the  $\Delta/\Delta$ KASH mice have irregularly shaped nuclei, with large invaginations of the nuclear membrane (Figure 6A, arrow). Approximately three-quarters (69%) of  $\Delta/\Delta$ KASH nuclei examined showed evidence of these invaginations, while in wildtype nuclei one-quarter (25%) had invaginations (66 of 96 and 17 of 69 nuclei for  $\Delta/\Delta$ KASH and wildtype, respectively). We also noted that the  $\Delta/\Delta$ KASH nuclei have a scarcity of electron-dense heterochromatin around the nuclear membrane. We measured a subset of the above nuclei for the amount of electron-dense material in each nucleus for both  $\Delta/\Delta$ KASH and wildtype littermates. Using Image J software, we measured the mean pixel intensity for each nucleus to measure the amount of electron-dense heterochromatin. The wildtype mice had significantly higher pixel intensity than  $\Delta/\Delta$ KASH mice ( $184.1 \pm 2.8$  vs.  $170.6 \pm 4.0$   $n=59$  and  $75$  nuclei, respectively,  $p=0.01$ ; wildtype and  $\Delta/\Delta$ KASH respectively), (Figure 6B). These data demonstrate that  $\Delta/\Delta$ KASH nuclei have a reduction in the total amount of heterochromatin.

## **DISCUSSION**

Mutations in components of the LINC complex, lamin A/C and emerin cause dilated cardiomyopathy with conduction system defects. Zhang and colleagues recently described variants in nesprin-1 and -2 that contribute to a range of phenotypes including dilated cardiomyopathy with conduction system defects with variable muscle disease [17]. We identified a patient with dilated cardiomyopathy with a nesprin-1 variant, R374H. The proband's father died at 61 years old from heart failure after having a pacing defibrillator implanted. Although the inherited nature of this DNA variant could not be demonstrated, its high conservation across species, protein positioning, and absence in 300 ethnically matched control chromosomes implicate the R374H nesprin-1 $\alpha$  variant in dilated cardiomyopathy. R374H nesprin-1 $\alpha$  fibroblasts were shown to have increased levels of nesprin-1 $\alpha$  and lamins A and C protein, indicating a perturbed LINC complex, strengthening the hypothesis that the R374H variant causes disease.

To further understand nesprin-1's role in dilated cardiomyopathy, we used the  $\Delta/\Delta$ KASH mouse model. The  $\Delta/\Delta$ KASH mouse has a functionally disrupted LINC complex due to the absence of the KASH domain that is known to interact with SUN2 in the perinuclear space [22]. In contrast, position 374 of nesprin-1 $\alpha$ , falls within the nucleoplasmic domain of nesprin-1 $\alpha$ . We hypothesize that the R374H mutation destabilizes the LINC complex possibly by altering the interaction with the inner nuclear membrane associated-intermediate filament network or through an interaction with other nuclear membrane components such as emerin. An altered inner nuclear membrane network may trigger compensatory upregulation of nesprin-1 and lamin A/C. This disruption in the LINC complex eventually leads to cardiac



disease. ECG analysis of the  $\Delta/\Delta$ KASH mice revealed an elongated P wave characteristic of atrial disease and affecting the conduction system. The P wave abnormality observed in both young (<32 weeks old) and old (>52 weeks old) mice indicates that cardiac defects may develop at even younger ages and precede the development of overt cardiomyopathy. It was also interesting to note that the QRS was elongated in the old  $\Delta/\Delta$ KASH male mice. The widened QRS may derive from cardiomyopathic changes or may reflect ventricular conduction defects. The sex difference observed here was unexpected, as male mice do not appear to have a more severe course of muscle disease in this model. It is possible that a larger study would have revealed QRS elongation in the females, as there is variability in the muscle phenotype.

$\Delta/\Delta$ KASH mice have further defects in myocardial conduction as evidenced by electrophysiologic studies.  $\Delta/\Delta$ KASH mice have a significantly longer atrial effective refractory period (AERP) compared to wildtype littermates indicating a conduction defect in the atrial myocytes. The ventricular effective refractory period (VERP) was not significantly different than wildtype in the old  $\Delta/\Delta$ KASH mice, however, there was a trend ( $p=0.06$ ) towards an elongated VERP. This trend was not evident in the young mice, but the AERP was different in young mice. These data reveal that the conduction defects of the myocardium in  $\Delta/\Delta$ KASH mice are progressive, similar to what is seen in patients with dilated cardiomyopathy arising from mutations in the LINC complex proteins. This same progression was evident during echocardiography studies. Young  $\Delta/\Delta$ KASH mice have normal fractional shortening, while old  $\Delta/\Delta$ KASH mice have reduced fractional shortening. This progressive reduction in systolic function is indicative of cardiomyopathy. It is also noteworthy that the  $\Delta/\Delta$ KASH mice do not exhibit overt dilation of the left ventricle, even at advanced age (data not shown); this could reflect altered mechanosensing and the ability of weakened heart to dilate or hypertrophy as a response. The lamin A/C component of the LINC complex has been implicated in mechanosensation [27].

We also noted abnormally elongated nuclei in the myocardium of  $\Delta/\Delta$ KASH mice. Elongated nuclei have been noted in the  $LMNA^{+/-}$  mouse model [26]. The  $LMNA^{+/-}$  mouse lacks one copy of *LMNA* and therefore genetically recapitulates the dominant *LMNA* mutations found in humans. The  $LMNA^{+/-}$  mouse exhibits dilated cardiomyopathy and cardiac conduction system disease [26,28]. Another mouse model with a homozygous mutation in *LMNA*, H222P, has also been described as a model for cardiomyopathy [29]. These mice also have abnormally elongated nuclei in their cardiomyocytes [25]. Recent work by Muchir and colleagues implicated the extracellular signal-regulated kinase (ERK) in the genesis of lamin A/C cardiomyopathy [25]. This finding argues that the LINC complex has an important signaling role in addition to its structural role in the nucleus.

The  $LMNA^{-/-}$  mouse completely lacks lamin A/C and develops rapidly progressive dilated cardiomyopathy with conduction system defects [30]. These mice have altered cardiomyocyte nuclear morphology with changes in heterochromatin organization. Abnormal heterochromatin has also been observed in hearts from patients with dilated cardiomyopathy as a result of mutations in lamin A/C [31,32]. The similar clinical and nuclear changes found in the  $\Delta/\Delta$ KASH mouse support that nesprin and lamin A/C function in the same pathway. While the lamins are known to affect gene regulation, it has always been hypothesized that nuclear defects were the result of stress on the cell. These new data may indicate that the nuclear shape defects are the result of aberrant signaling. The relationship between these signals and mechanical defects requires further investigation to determine if they result of nuclear membrane weakness and/or direct gene expression alterations.

## Supplementary Material

Refer to Web version on PubMed Central for supplementary material.

## Acknowledgments

Supported by NIH HL092443 (to EMM) and the Doris Duke Charitable Foundation.

## ABBREVIATIONS

DCM	dilated cardiomyopathy
EDMD	Emery Dreifuss muscular dystrophy
ECG	electrocardiogram
AERP	atrial effective refractory period
VERP	ventricular effective refractory period
ECG	electrocardiogram
FS	fractional shortening

## REFERENCES

- [1]. Crisp M, Liu Q, Roux K, Rattner JB, Shanahan C, Burke B, Stahl PD, Hodzic D. Coupling of the nucleus and cytoplasm: role of the LINC complex. *J Cell Biol* 2006;172:41–53. [PubMed: 16380439]
- [2]. Stewart-Hutchinson PJ, Hale CM, Wirtz D, Hodzic D. Structural requirements for the assembly of LINC complexes and their function in cellular mechanical stiffness. *Exp Cell Res* 2008;314:1892–905. [PubMed: 18396275]
- [3]. Padmakumar VC, Libotte T, Lu W, Zaim H, Abraham S, Noegel AA, Gotzmann J, Foisner R, Karakesisoglou I. The inner nuclear membrane protein Sun1 mediates the anchorage of Nesprin-2 to the nuclear envelope. *J Cell Sci* 2005;118:3419–30. [PubMed: 16079285]
- [4]. Haque F, Lloyd DJ, Smallwood DT, Dent CL, Shanahan CM, Fry AM, Trembath RC, Shackleton S. SUN1 interacts with nuclear lamin A and cytoplasmic nesprins to provide a physical connection between the nuclear lamina and the cytoskeleton. *Mol Cell Biol* 2006;26:3738–51. [PubMed: 16648470]
- [5]. Ivorra C, Kubicek M, Gonzalez JM, Sanz-Gonzalez SM, Alvarez-Barrientos A, O'Connor JE, Burke B, Andres V. A mechanism of AP-1 suppression through interaction of c-Fos with lamin A/C. *Genes Dev* 2006;20:307–20. [PubMed: 16452503]
- [6]. Lammerding J, Lee RT. The nuclear membrane and mechanotransduction: impaired nuclear mechanics and mechanotransduction in lamin A/C deficient cells. *Novartis Found Symp* 2005;264:264–73. discussion 273–8. [PubMed: 15773759]
- [7]. Favreau C, Dubosclard E, Ostlund C, Vigouroux C, Capeau J, Wehnert M, Higuier D, Worman HJ, Courvalin JC, Buendia B. Expression of lamin A mutated in the carboxyl-terminal tail generates an aberrant nuclear phenotype similar to that observed in cells from patients with Dunnigan-type partial lipodystrophy and Emery-Dreifuss muscular dystrophy. *Exp Cell Res* 2003;282:14–23. [PubMed: 12490190]
- [8]. Taylor MR, Fain PR, Sinagra G, Robinson ML, Robertson AD, Carniel E, Di Lenarda A, Bohlmeier TJ, Ferguson DA, Brodsky GL, Boucek MM, Lascor J, Moss AC, Li WL, Stetler GL, Muntoni F, Bristow MR, Mestroni L. Natural history of dilated cardiomyopathy due to lamin A/C gene mutations. *J Am Coll Cardiol* 2003;41:771–80. [PubMed: 12628721]
- [9]. Sanna T, Dello Russo A, Toniolo D, Vytöpil M, Pelargonio G, De Martino G, Ricci E, Silvestri G, Giglio V, Messano L, Zachara E, Bellocchi F. Cardiac features of Emery-Dreifuss muscular dystrophy caused by lamin A/C gene mutations. *Eur Heart J* 2003;24:2227–36. [PubMed: 14659775]
- [10]. van Berlo JH, de Voogt WG, van der Kooij AJ, van Tintelen JP, Bonne G, Yaou RB, Duboc D, Rossenbacker T, Heidebuchel H, de Visser M, Crijns HJ, Pinto YM. Meta-analysis of clinical characteristics of 299 carriers of LMNA gene mutations: do lamin A/C mutations portend a high risk of sudden death? *J Mol Med* 2005;83:79–83. [PubMed: 15551023]

- [11]. Arbustini E, Pilotto A, Repetto A, Grasso M, Negri A, Diegoli M, Campana C, Scelsi L, Baldini E, Gavazzi A, Tavazzi L. Autosomal dominant dilated cardiomyopathy with atrioventricular block: a lamin A/C defect-related disease. *J Am Coll Cardiol* 2002;39:981–90. [PubMed: 11897440]
- [12]. Bonne G, Yaou RB, Beroud C, Boriani G, Brown S, de Visser M, Duboc D, Ellis J, Hausmanowa-Petrusewicz I, Lattanzi G, Merlini L, Morris G, Muntoni F, Opolski G, Pinto YM, Sangiuolo F, Toniolo D, Trembath R, van Berlo JH, van der Kooi AJ, Wehnert M. 108th ENMC International Workshop, 3rd Workshop of the MYO-CLUSTER project: EUROMEN, 7th International Emery-Dreifuss Muscular Dystrophy (EDMD) Workshop, 13–15 September 2002, Naarden, The Netherlands. *Neuromuscul Disord* 2003;13:508–15. [PubMed: 12899879]
- [13]. Meune C, Van Berlo JH, Anselme F, Bonne G, Pinto YM, Duboc D. Primary prevention of sudden death in patients with lamin A/C gene mutations. *N Engl J Med* 2006;354:209–10. [PubMed: 16407522]
- [14]. Lee KK, Haraguchi T, Lee RS, Koujin T, Hiraoka Y, Wilson KL. Distinct functional domains in emerin bind lamin A and DNA-bridging protein BAF. *J Cell Sci* 2001;114:4567–73. [PubMed: 11792821]
- [15]. Haraguchi T, Koujin T, Segura-Totten M, Lee KK, Matsuoka Y, Yoneda Y, Wilson KL, Hiraoka Y. BAF is required for emerin assembly into the reforming nuclear envelope. *J Cell Sci* 2001;114:4575–85. [PubMed: 11792822]
- [16]. Holaska JM. Emerin and the nuclear lamina in muscle and cardiac disease. *Circ Res* 2008;103:16–23. [PubMed: 18596264]
- [17]. Zhang Q, Bethmann C, Worth NF, Davies JD, Wasner C, Feuer A, Ragnauth CD, Yi Q, Mellad JA, Warren DT, Wheeler MA, Ellis JA, Skepper JN, Vorgerd M, Schlotter-Weigel B, Weissberg PL, Roberts RG, Wehnert M, Shanahan CM. Nesprin-1 and -2 are involved in the pathogenesis of Emery Dreifuss muscular dystrophy and are critical for nuclear envelope integrity. *Hum Mol Genet* 2007;16:2816–33. [PubMed: 17761684]
- [18]. Zhang Q, Skepper JN, Yang F, Davies JD, Hegyi L, Roberts RG, Weissberg PL, Ellis JA, Shanahan CM. Nesprins: a novel family of spectrin-repeat-containing proteins that localize to the nuclear membrane in multiple tissues. *J Cell Sci* 2001;114:4485–98. [PubMed: 11792814]
- [19]. Apel ED, Lewis RM, Grady RM, Sanes JR. Syne-1, a dystrophin- and Klarsicht-related protein associated with synaptic nuclei at the neuromuscular junction. *J Biol Chem* 2000;275:31986–95. [PubMed: 10878022]
- [20]. Zhen YY, Libotte T, Munck M, Noegel AA, Korenbaum E. NUANCE, a giant protein connecting the nucleus and actin cytoskeleton. *J Cell Sci* 2002;115:3207–22. [PubMed: 12118075]
- [21]. Mislow JM, Kim MS, Davis DB, McNally EM. Myne-1, a spectrin repeat transmembrane protein of the myocyte inner nuclear membrane, interacts with lamin A/C. *J Cell Sci* 2002;115:61–70. [PubMed: 11801724]
- [22]. Puckelwartz MJ, Kessler E, Zhang Y, Hodzic D, Randles KN, Morris G, Earley JU, Hadhazy M, Holaska JM, Mewborn SK, Pytel P, McNally EM. Disruption of nesprin-1 produces an Emery Dreifuss muscular dystrophy-like phenotype in mice. *Hum Mol Genet* 2009;18:607–20. [PubMed: 19008300]
- [23]. McNally EM, Passos-Bueno MR, Bonnemann CG, Vainzof M, de Sa Moreira E, Lidov HG, Othmane KB, Denton PH, Vance JM, Zatz M, Kunkel LM. Mild and severe muscular dystrophy caused by a single gamma-sarcoglycan mutation. *Am J Hum Genet* 1996;59:1040–7. [PubMed: 8900232]
- [24]. Mislow JM, Holaska JM, Kim MS, Lee KK, Segura-Totten M, Wilson KL, McNally EM. Nesprin-1alpha self-associates and binds directly to emerin and lamin A in vitro. *FEBS Lett* 2002;525:135–40. [PubMed: 12163176]
- [25]. Muchir A, Shan J, Bonne G, Lehnart SE, Worman HJ. Inhibition of extracellular signal-regulated kinase signaling to prevent cardiomyopathy caused by mutation in the gene encoding A-type lamins. *Hum Mol Genet* 2009;18:241–7. [PubMed: 18927124]
- [26]. Wolf CM, Wang L, Alcalai R, Pizard A, Burgon PG, Ahmad F, Sherwood M, Branco DM, Wakimoto H, Fishman GI, See V, Stewart CL, Conner DA, Berul CI, Seidman CE, Seidman JG. Lamin A/C haploinsufficiency causes dilated cardiomyopathy and apoptosis-triggered cardiac conduction system disease. *J Mol Cell Cardiol* 2008;44:293–303. [PubMed: 18182166]

- [27]. Lammerding J, Schulze PC, Takahashi T, Kozlov S, Sullivan T, Kamm RD, Stewart CL, Lee RT. Lamin A/C deficiency causes defective nuclear mechanics and mechanotransduction. *J Clin Invest* 2004;113:370–8. [PubMed: 14755334]
- [28]. Sullivan T, Escalante-Alcalde D, Bhatt H, Anver M, Bhat N, Nagashima K, Stewart CL, Burke B. Loss of A-type lamin expression compromises nuclear envelope integrity leading to muscular dystrophy. *J Cell Biol* 1999;147:913–20. [PubMed: 10579712]
- [29]. Arimura T, Helbling-Leclerc A, Massart C, Varnous S, Niel F, Lacene E, Fromes Y, Toussaint M, Mura AM, Keller DI, Amthor H, Isnard R, Malissen M, Schwartz K, Bonne G. Mouse model carrying H222P-Lmna mutation develops muscular dystrophy and dilated cardiomyopathy similar to human striated muscle laminopathies. *Hum Mol Genet* 2005;14:155–69. [PubMed: 15548545]
- [30]. Nikolova V, Leimena C, McMahon AC, Tan JC, Chandar S, Jogia D, Kesteven SH, Michalick J, Otway R, Verheyen F, Rainer S, Stewart CL, Martin D, Feneley MP, Fatkin D. Defects in nuclear structure and function promote dilated cardiomyopathy in lamin A/C-deficient mice. *J Clin Invest* 2004;113:357–69. [PubMed: 14755333]
- [31]. Fidzianska A, Bilinska ZT, Tesson F, Wagner T, Walski M, Grzybowski J, Ruzyllo W, Hausmanowa-Petrusewicz I. Obliteration of cardiomyocyte nuclear architecture in a patient with LMNA gene mutation. *J Neurol Sci* 2008;271:91–6. [PubMed: 18502446]
- [32]. Sylvius N, Bilinska ZT, Veinot JP, Fidzianska A, Bolongo PM, Poon S, McKeown P, Davies RA, Chan KL, Tang AS, Dyack S, Grzybowski J, Ruzyllo W, McBride H, Tesson F. In vivo and in vitro examination of the functional significances of novel lamin gene mutations in heart failure patients. *J Med Genet* 2005;42:639–47. [PubMed: 16061563]

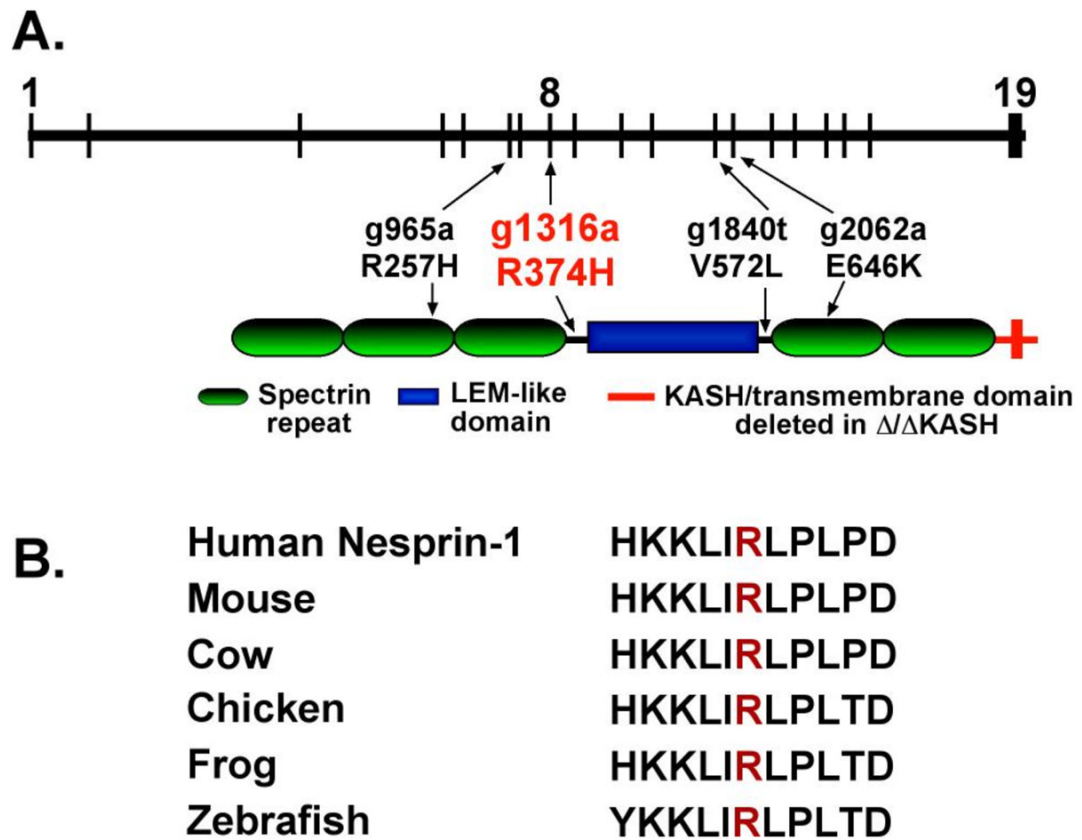


**Figure 1. Nesprin-1 R374H in an individual with nonischemic dilated cardiomyopathy**  
 (A) Schematic representation of the gene structure (top) and protein structure (bottom) of nesprin-1 $\alpha$ , an isoform of nesprin-1 highly expressed in cardiac and skeletal muscle. The vertical lines indicate the positioning of nesprin-1 $\alpha$  exons within the gene. A sequence variant (g1316a) was identified in a patient with dilated cardiomyopathy (red). The variant maps to a conserved region between a spectrin repeat and the LEM-like domain in the protein. Variants previously identified by Zhang and colleagues are shown in black [17]. (B) The R374H variant is conserved across vertebrate species.

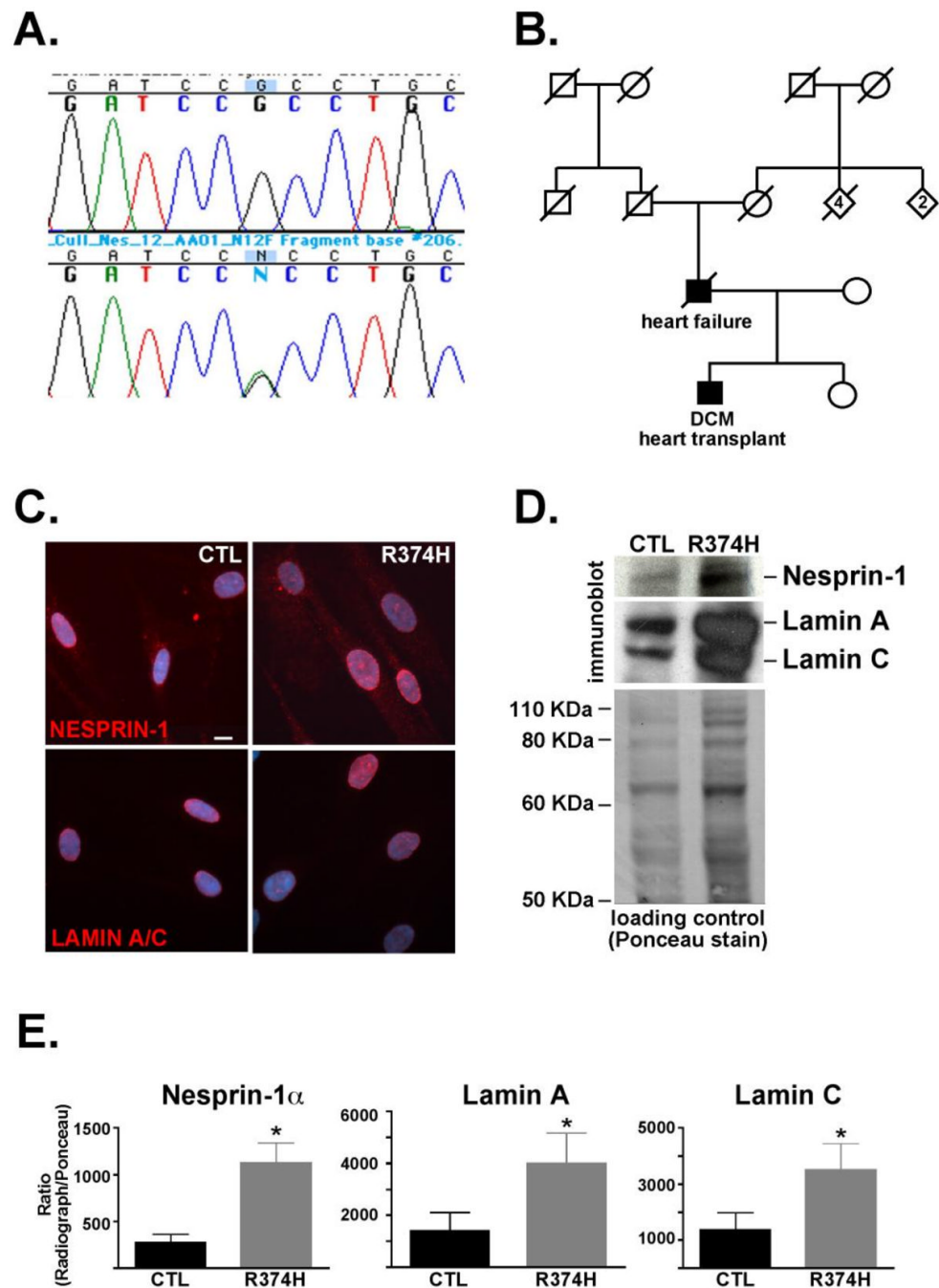


**Figure 2. Dilated cardiomyopathy with nesprin-1 $\alpha$  R374H**

(A) Sequence analysis from the proband's DNA revealed a heterozygous G to A change at nucleotide 1316 in nesprin-1 $\alpha$ . The G1361A change is predicted to result in an amino acid change, R374H, in nesprin-1 $\alpha$ . (B) Pedigree from proband carrying the R374H variant. The proband and his father were both affected (black). (C) Human fibroblasts from the nesprin-1 $\alpha$  R374H patient and a control cell line (CTL) were analyzed by immunofluorescence microscopy using antibodies for nesprin-1 and lamin A/C. DAPI shows nuclei. Scale bar=10 $\mu$ m (D) Immunoblotting was performed on human fibroblasts from the nesprin-1 $\alpha$  R374H and control (CTL) using antibodies to nesprin-1 and lamin A/C. Ponceau staining is shown as loading control. (E) Densitometry was performed. The ratio of LINC components

nesprin1- $\alpha$  and lamins A and C were normalized to loading control and averaged over 3 experiments,  $p < 0.05$ .

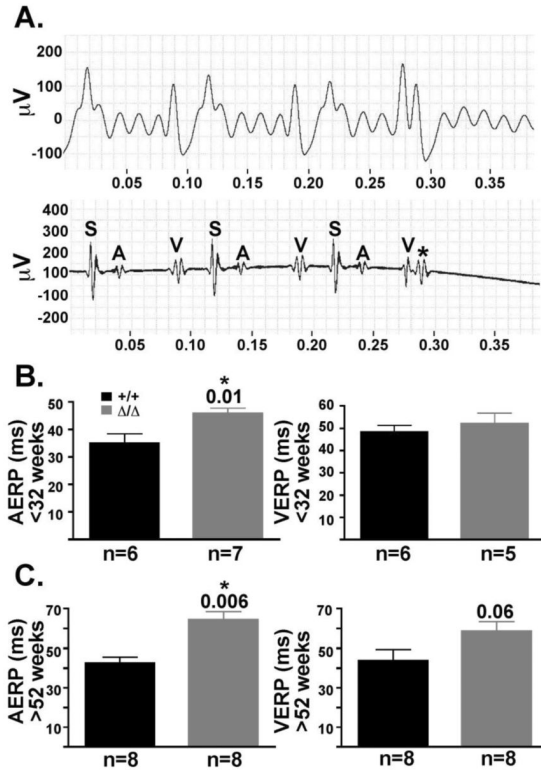


**Figure 3.  $\Delta/\Delta$ KASH mice have prolonged refractory times affecting the atrial and ventricles compared to wildtype littermates**

(A) Representative surface ECG (top) and corresponding intracardiac electrophysiologic (bottom) tracing from  $\Delta/\Delta$ KASH mouse. The pacing stimulus is labeled S, the atrial response A and the ventricular response V. At 60ms, the  $\Delta/\Delta$ KASH heart has no atrial response to an early stimulus, shown by the asterisk. (B) Graphs of the AERP and VERP in young (<32 weeks) and (C) old (>52 weeks)  $\Delta/\Delta$ KASH mice and wildtype littermates. Both young and old  $\Delta/\Delta$ KASH mice have a longer AERP (p=0.01 and p=0.006, respectively) and a slightly longer VERP (p=0.06) than wildtype littermates. Black bars represent wildtype mice, gray bars represent  $\Delta/\Delta$ KASH mice. Number of mice in each study are listed below the corresponding bars. ms=milliseconds



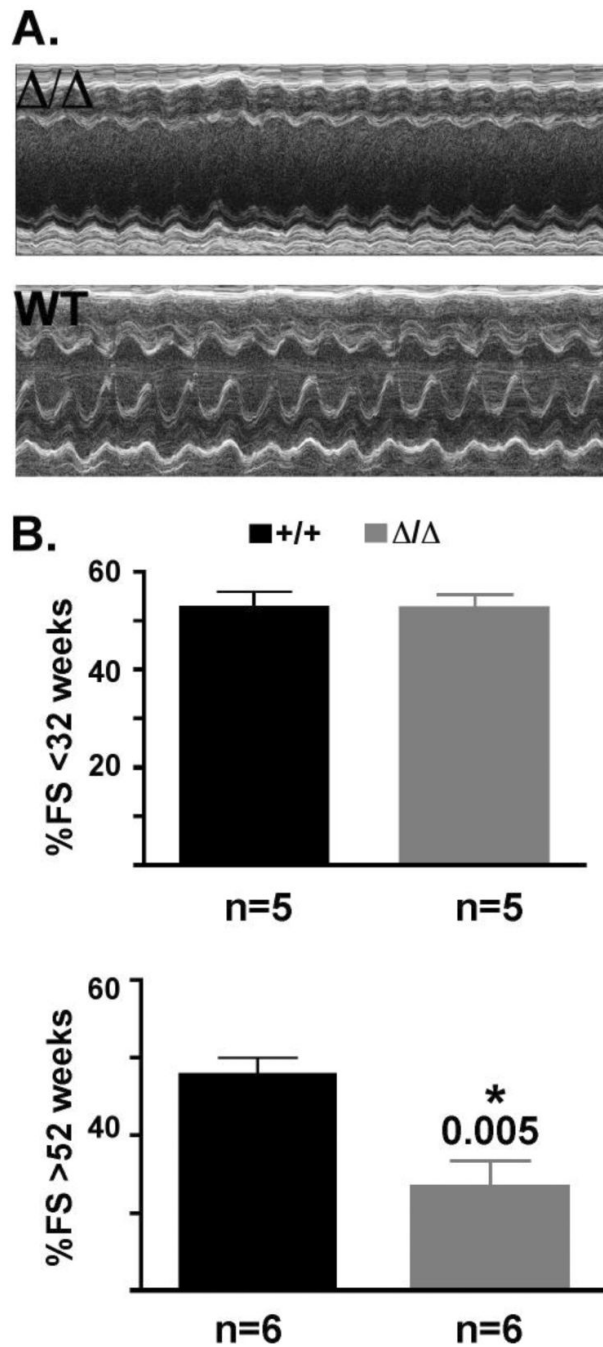


**Figure 4.  $\Delta/\Delta$ KASH mice have reduced fractional shortening compared to wildtype littermates** (A) Representative m-mode echocardiography from an old (>52 weeks)  $\Delta/\Delta$ KASH mouse and wildtype littermate showing reduced fractional shortening. (B) Graphs of fractional shortening in <32 week old (top) and >52 week old (bottom)  $\Delta/\Delta$ KASH mice (gray bar) and wildtype littermates (black bar). Number of animals tested shown at bottom under bar.

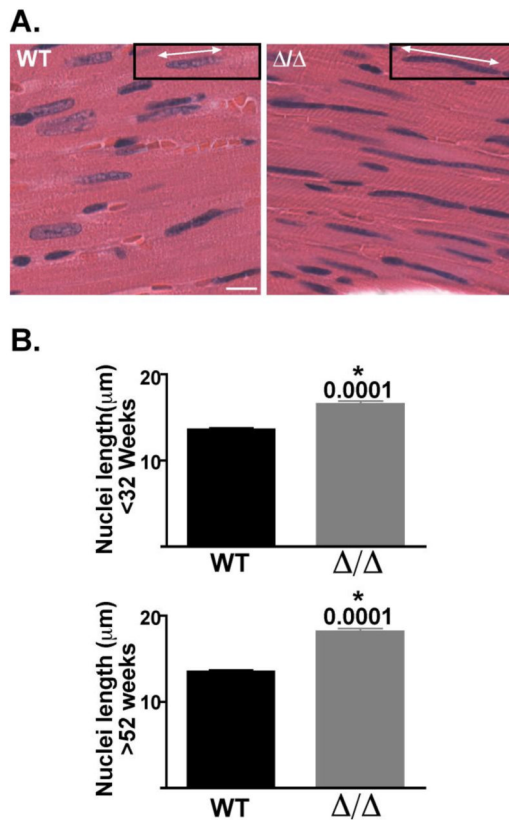


**Figure 5.  $\Delta/\Delta$ KASH mice have abnormally shaped cardiomyocyte nuclei compared to wildtype littermates**

(A) Histological analysis of coronal sections of hearts from >52 week old  $\Delta/\Delta$ KASH mice and wildtype littermates. Hematoxylin and eosin stained wildtype sections have rounded nuclei, while  $\Delta/\Delta$ KASH sections have elongated cardiomyocyte nuclei. Insets with white arrows demonstrate the measurement of nuclear length. Scale bar: 10 $\mu$ m. (B) Quantification of nuclear elongation in <32 week old mice (top) and >52 week old mice (bottom)  $\Delta/\Delta$ KASH (gray bar) and wildtype littermates (black bar).  $\Delta/\Delta$ KASH mice in both age groups have elongated cardiomyocyte nuclei (p=0.0001). Three animals each genotype, each age were counted, approximately 100 nuclei per animal.

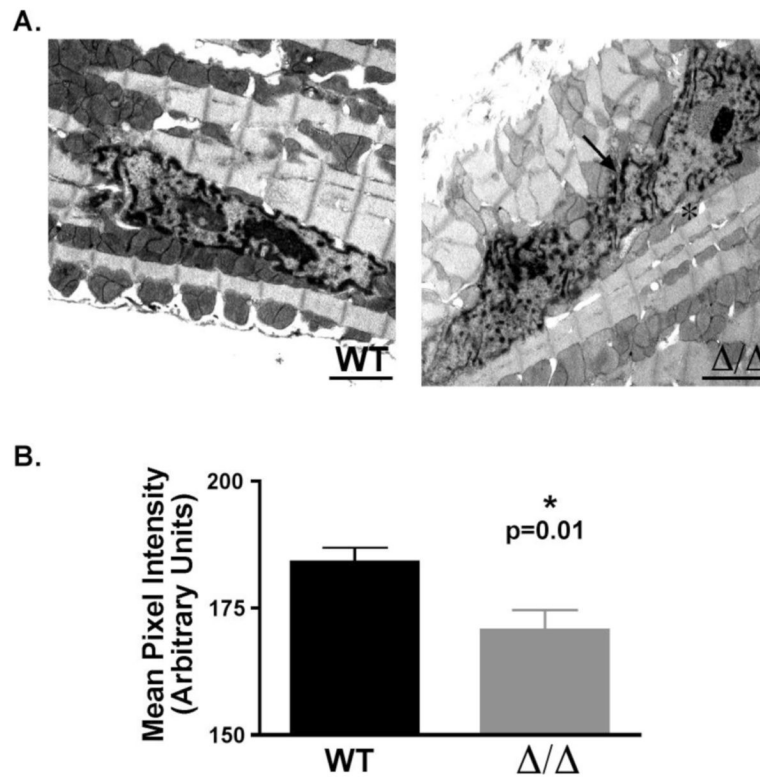


**Figure 6. The  $\Delta/\Delta$ KASH cardiomyocyte nucleus is abnormally shaped and has thinner heterochromatin layer**

(A) Electron microscopy was performed on longitudinal sections of hearts from <32 week old  $\Delta/\Delta$ KASH and wildtype littermates.  $\Delta/\Delta$ KASH cardiomyocyte nuclei are irregularly shaped with invaginations of the nuclear membrane (arrow) and reduced heterochromatin at the nuclear membrane (asterisk). (B) Quantification the amount of electron-dense heterochromatin in the nucleus. Wildtype nuclei have significantly more heterochromatin in their nuclei compared to  $\Delta/\Delta$ KASH mice measured as pixel intensity of the electron dense regions in the nucleus, n=59 and 75 nuclei for wildtype and  $\Delta/\Delta$ KASH mice respectively (p=0.01).

Table 1

ECG data from  $\Delta/\Delta$ KASH and WT mice

<32 weeks					
	QRS	p	QTc	p	P duration
$\Delta/\Delta$ KASH	16.3±1.7 (5)	NS	101.9±26.8 (5)	NS	23.8±1.4 (6)
Wildtype	17.0±2.3 (6)		84.1 ±4.5 (6)		17.3±0.5 (6)
					0.0009

<52 weeks					
	QRS	p	QTc	p	P duration
$\Delta/\Delta$ KASH	16.8±1.3 (9)	NS	88.6±10.2 (9)	NS	21.4±2.1 (8)
Wildtype	14.6±1.2 (8)		84.7±14.5 (8)		15.6±1.0 (8)
					0.03